

The cooperative effect of aromatic ring stacking and Pt(II)- π -phosphate and π -phosphate polar bonds explains the strong intercalative DNA binding by platinum intercalators³ and Ru-(phen)₃²⁺.³⁵ The Pt(II) center has an electron-withdrawing effect

on L which is similar to that of the positively charged nitrogen of typical intercalators such as ethidium bromide. Detailed calorimetric studies are being carried out in this laboratory, and they will enable us to have a deeper insight into the thermodynamic aspects of the adduct formation.

- (35) (a) Barton, J. K.; Danishefsky, A. T.; Goldberg, J. M. *J. Am. Chem. Soc.* **1984**, *106*, 2172-2176. (b) Barton, J. K.; Goldberg, J. M.; Kuma, C. V.; Turro, N. J. *J. Am. Chem. Soc.* **1986**, *108*, 2081-2088. (c) Barton, J. K. *Science* **1986**, *233*, 727-734.

Acknowledgment. This work was supported by a Grant-in-Aid for Scientific Research by the Ministry of Education, Science, and Culture of Japan, to which our thanks are due.

Contribution from the Department of Chemistry, University of Washington, Seattle, Washington 98195

Oxygen Atom Transfer from a Phosphine Oxide to Tungsten(II) Compounds

Stephanie L. Brock and James M. Mayer*¹

Received November 13, 1990

WCl₂(PMePh₂)₄ (**1**) reacts rapidly with Ph₂P(O)CH₂CH₂PPh₂ (**5**, the monooxide of diphos) to give an adduct, WCl₂[Ph₂P(O)CH₂CH₂PPh₂](PMePh₂)₂ (**6**). On being heated at 80 °C for 8 h, **6** rearranges by transferring the phosphoryl oxygen to tungsten, with the formation of tungsten-oxo complexes W(O)Cl₂(diphos)(PMePh₂) (**7**) and W(O)Cl₂(PMePh₂)₃ (**2**), as well as WCl₂(diphos)(PMePh₂)₂ (**8**). This is the first example of oxygen atom transfer from a phosphine oxide to a metal center, a remarkable reaction because of the strength of the P-O bond (roughly 130 kcal/mol). The presence of an oxygen atom transfer step in this reaction has been confirmed by oxygen-18-labeling studies. WCl₂(PMe₃)₄ (**9**) also deoxygenates **5**, forming similar tungsten-oxo complexes, but in this case an intermediate is not observed. Nonchelating phosphine oxides are unreactive with **1** and **9**, indicating that the chelating nature of **5** is needed to assist the initial coordination of the phosphoryl oxygen. The kinetic barriers to deoxygenation of phosphine oxides lie both in the initial coordination of the phosphine oxide and in the actual oxygen atom transfer step. Allyl- and vinylphosphine oxides also react with **1**, but oxygen atom transfer from these substrates has not been observed. An unusual tungsten-oxo complex with a chelating allyldiphenylphosphine oxide, W(O)Cl₂[CH₂=CHCH₂P(O)Ph₂](PMePh₂) (**13**) has been isolated and its X-ray crystal structure determined. Crystal data for **13**: *a* = 9.2547 (9) Å, *b* = 16.738 (2) Å, *c* = 18.023 (2) Å, β = 100.696 (9)°, monoclinic, *P*2₁/*c*, *Z* = 4.

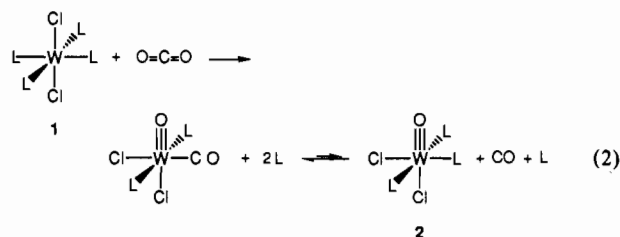
Oxygen atom transfer reactions have received increasing attention in recent years because of their importance as fundamental steps in a variety of both stoichiometric and catalytic processes.²⁻⁴ Examples range from the reduction of nitrate to nitrite mediated by a molybdenum enzyme⁵ to the epoxidation of olefins by a number of metal-oxo complexes, including the iron-oxo center in cytochrome P-450 enzymes.⁶ A variety of reagents have been used to deliver an oxygen atom to a metal center or remove oxygen from a metal.^{2,3} By far, the most common reagents for oxygen atom abstraction are phosphines, PR₃, which reduce a wide range of metal-oxo complexes (eq 1).



The reactivity of phosphines results in large part from the very strong P-O bond, 127 kcal/mol in Ph₃PO and 139 kcal/mol in Me₃PO.⁷ Because of this strong bond, the oxidation of phosphines is easy to accomplish, while only strongly reducing reagents will generate phosphines from phosphine oxides (e.g., LiAlH₄, PhSiH₃).⁸ The reactions reported here are the first examples

of oxygen atom transfer from a phosphine oxide to a metal complex, the reverse of eq 1.⁹

Our studies of WCl₂(PMePh₂)₄ (**1**) have shown it to be an extremely potent oxygen atom acceptor, forming oxo complexes on reaction with water, alcohols, ketones, epoxides, SO₂, and CO₂.¹⁰⁻¹³ The cleavage of CO₂ forms an equilibrium mixture of the oxo-carbonyl and oxo-tris(phosphine) complexes, W(O)Cl₂(CO)(PMePh₂)₂ and W(O)Cl₂(PMePh₂)₃ (eq 2),^{10,11,14} a re-



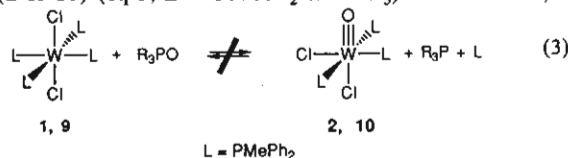
markable reaction because of the strength of the C-O bond that

- (1) Presidential Young Investigator, 1988-1993; Alfred P. Sloan Research Fellow, 1989-1991.
 (2) Holm, R. H. *Chem. Rev.* **1987**, *87*, 1401-1449.
 (3) Nugent, W. A.; Mayer, J. M. *Metal-Ligand Multiple Bonds*; Wiley-Interscience: New York, 1988; pp 248-251.
 (4) Sheldon, R. A.; Kochi, J. K. *Metal-Catalyzed Oxidations of Organic Compounds*; Academic: New York, 1981.
 (5) *Molybdenum Enzymes*; Spiro, T. G., Ed.; Wiley-Interscience: New York, 1985. Model studies: Craig, J. A.; Holm, R. H. *J. Am. Chem. Soc.* **1989**, *111*, 2111-2115. Garner, C. D.; Hyde, M. R.; Mabbs, F. E.; Routledge, V. I. *J. Chem. Soc., Dalton Trans.* **1975**, 1180-1186. Wiegardt, K.; Woeste, M.; Roy, P. S.; Chaudhuri, P. *J. Am. Chem. Soc.* **1985**, *107*, 8276-8277.
 (6) *Cytochrome P-450 Structure, Mechanism, and Biochemistry*; Ortiz de Montellano, P. R., Ed.; Plenum: New York, 1986; see especially Chapter 1.
 (7) Hudson, R. F. *Structure and Mechanism in Organo-Phosphorus Chemistry*; Academic: New York, 1965; pp 68-70.

- (8) Hays, H. R.; Peterson, D. J. In *Organic Phosphorus Compounds*; Kocolapoff, G. M., Maier, L., Eds.; Wiley: New York, 1972; Vol. 3, pp 408-413.
 (9) There are examples of oxide (O²⁻) transfer from a phosphine oxide to a metal, without oxidation state changes. See, for instance: Horner, S. M.; Tyree, S. Y., Jr. *Inorg. Chem.* **1962**, *1*, 122-127.
 (10) Su, F. M.; Bryan, J. C.; Jang, S.; Mayer, J. M. *Polyhedron* **1989**, *8*, 1261-1277.
 (11) Bryan, J. C.; Geig, S. J.; Rheingold, A. L.; Mayer, J. M. *J. Am. Chem. Soc.* **1987**, *109*, 2826-2828.
 (12) Bryan, J. C.; Mayer, J. M. *J. Am. Chem. Soc.* **1990**, *112*, 2298-2308.
 (13) Jang, S.; Atagi, L. M.; Mayer, J. M. *J. Am. Chem. Soc.* **1990**, *112*, 6413-6414.
 (14) The equilibrium W(O)Cl₂(CO)(PMePh₂)₂ + PMePh₂ ⇌ W(O)Cl₂(PMePh₂)₃ + CO lies to the left; *K*_{eq} has been estimated to be 500.

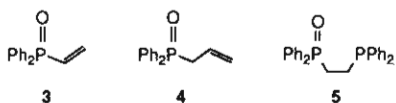
is broken, 127 kcal/mol.¹² Because the P–O bond strength in Ph₃PO is equal to the C–O bond strength in CO₂, the deoxygenation of Ph₃PO is also likely to be thermodynamically favorable.¹⁵ However, Ph₃PO is not deoxygenated by **1** or by WCl₂(PMe₃)₄ (**9**).

There must be a kinetic barrier to oxygen atom transfer between phosphorus and tungsten in this system, since **1** and **9** do not reduce simple phosphine oxides and phosphines will not reduce W(O)–Cl₂L₃ (**2** or **10**) (eq 3; L = PMePh₂ or PMe₃). In contrast, **1**



readily reduces very similar reagents: arsine oxides (Ph₃AsO), phosphine sulfides (Ph₂MePS), and phosphine imides (Ph₂MePNC₆H₄Me).¹⁰ This indicates that the barrier is not steric in origin—Ph₂MePNC₆H₄Me is certainly more bulky than Ph₂MePO.

Our original hypothesis was that the kinetic barrier to reduction of phosphine oxides arises from the difficulty in forming an initial complex between tungsten and R₃PO. The tungsten center in **1** is very electron rich and prefers “soft” ligands such as phosphines or alkenes,¹⁶ while phosphine oxides are very “hard” donors (R₃P=O ↔ R₃P⁺–O[–]), harder than analogous phosphine sulfides or phosphine imides. One way to circumvent this problem, if this is the origin of the kinetic barrier, is to attach the phosphine oxide to a better ligand for tungsten(II) and thereby favor its coordination by chelation. We have therefore studied the reactions of **1** and **9** with vinyl-, allyl-, and phosphine-substituted phosphine oxides, compounds **3–5**. We report here that both **4** and **5** can



act as chelating ligands to tungsten and that reaction of **5** with **1** or **9** (Scheme 1, eq 7) ultimately occurs by oxygen atom transfer to give tungsten(IV)–oxo complexes and Ph₂PCH₂CH₂PPh₂ (1,2-bis(diphenylphosphino)ethane, abbreviated diphos).

Results

WCl₂(PMePh₂)₄ (**1**) reacts with the functionalized phosphine oxides **3–5** within time of mixing in benzene to give ruby red solutions. The reaction with **5** gives primarily a single product containing 1 equiv of the phosphine oxide (**6**; see below), whereas **3** and **4** form mixtures of tungsten products. The reaction mixtures are stable for days at ambient temperatures in sealed tubes. At 80 °C, the reactions with **3** and **4** yield uncharacterized paramagnetic products; heating the reaction with **5**, however, results in deoxygenation of the phosphine oxide.

The reaction of **1** and **5** in C₆D₆ over 8 h at 80 °C gives three tungsten products: the oxo–diphos complex **7**, the oxo–tris(phosphine) species **2**,¹⁷ and a tungsten(II)–diphos complex **8** (Scheme 1). Compound **7** is the predominant product of the reaction and can be the sole product depending on the conditions. Diphos is the product of deoxygenation of **5**; it can be observed bound to the tungsten(IV) and tungsten(II) species in solution because it is a better ligand than either **5** or PMePh₂. Compounds **7** and **8** are independently prepared by substitution of two of the phosphine ligands in **2** or **1** with diphos, both facile reactions.¹⁸

Scheme 1

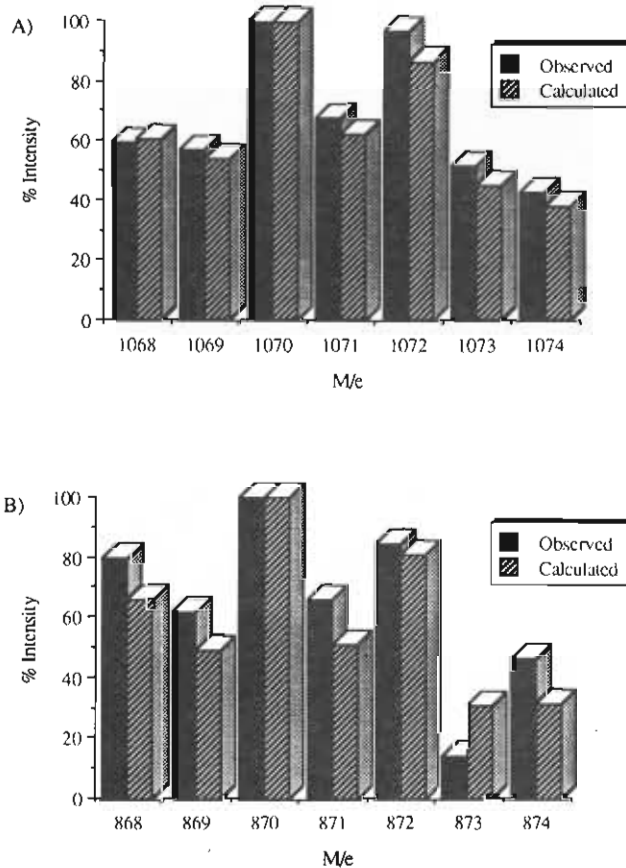
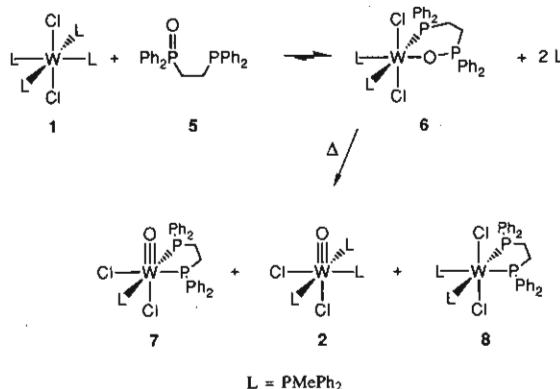


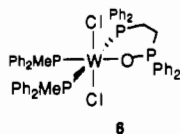
Figure 1. Observed and calculated intensities in the parent ion region of the FAB mass spectra for (A) WCl₂[Ph₂P(O)CH₂CH₂PPh₂](PMePh₂)₂ (**6**) and (B) W(*O)Cl₂(PMePh₂)(Ph₂PCH₂CH₂PPh₂) (**7**), where *O is 60% ¹⁸O, 40% ¹⁶O.

The conversion of **1** and **5** to the oxo complexes **2** and **7** clearly occurs by oxygen atom transfer from phosphorus to tungsten. Oxidation by adventitious air or moisture can be ruled out by the observed stoichiometry: the quantity of oxo products (**7** + **2**) is always close to the amount of diphos products formed (**7** + **8**). In one procedure, for example, NMR integration showed 7:2:8 = 6.5:1.5:1, an 8:7.5 ratio of oxo to diphos products. Oxygen atom transfer was also confirmed by an ¹⁸O-labeling study. ⁵⁻¹⁸O was prepared with 60% enrichment by the addition of bromine to diphos in the presence of H₂¹⁸O, followed by chromatography on silica gel. The oxo complexes produced from ⁵⁻¹⁸O and **1** are of comparable enrichment, as shown by IR spectra and FAB mass spectra (Figure 1). The tungsten–oxo stretch of 947 cm^{–1} in **7** shifts to 893 cm^{–1} on ¹⁸O substitution, close to the 50-cm^{–1} shift predicted for a harmonic oscillator.

The initial product of the reaction of **1** and **5** has been isolated as a red powder and determined to be a tungsten(II) complex of **5**, WCl₂[Ph₂P(O)CH₂CH₂PPh₂](PMePh₂)₂ (**6**), on the basis of

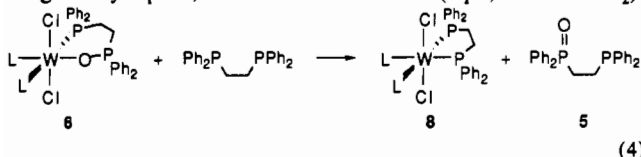
- (15) The stronger binding of CO vs PMePh₂¹⁴ to tungsten makes the deoxygenation of CO₂ more favorable than Ph₃PO by about 3 kcal/mol.
- (16) The known phosphine oxide complexes of tungsten(II) also contain carbonyl ligands and are therefore not as electron rich as **1** and **9**: Baker, P. K.; Kendrick, D. *J. Coord. Chem.* **1988**, *17*, 355–358. Planinic, P.; Meider, H. *Polyhedron* **1990**, *9*, 1099–1105.
- (17) Butcher, A. V.; Chatt, J.; Leigh, G. J.; Richards, P. L. *J. Chem. Soc., Dalton Trans.* **1972**, 1064–1069. Carmona, E.; Sanchez, L.; Poveda, M. L.; Jones, R. A.; Hefner, J. G. *Polyhedron* **1983**, *2*, 797–801. Chiu, K. W.; Lyons, D.; Wilkinson, G.; Thornton-Pett, M.; Hursthouse, M. B. *Polyhedron* **1983**, *2*, 803–810.
- (18) Atagi, L. Unpublished results.

its spectral data and its reactivity. It exhibits a complex ^1H NMR spectrum in C_6D_6 , with relatively sharp resonances from $\delta +25$ to -8 . Such sharp, shifted NMR spectra are characteristic of paramagnetic d^4 octahedral compounds of second- and third-row transition metals.¹⁹ The spectra are sufficiently sharp that coupling is observed in most of the resonances for meta (doublets) and para protons (triplets). While the chemical shifts are difficult to interpret, the presence of the "internal shift reagent" is very valuable. Since there is little overlapping among the 16 resonances predicted for **6**, it is clear that there are four different types of phenyl groups, two methylene resonances (δ 24.2, -7.2), and two inequivalent phosphine methyl groups (δ 9.31, -4.26). These data imply a C_2 structure, with cis-phosphine and trans-chloride ligands (as in the structure of **1**¹⁰):

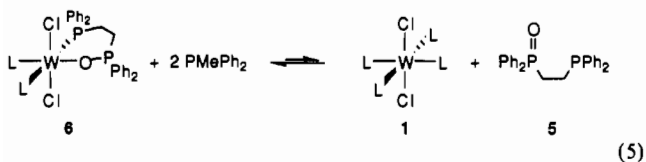


The IR spectrum of **6** shows a strong P–O stretching mode at 1167 cm^{-1} , which shifts to 1146 cm^{-1} on ^{18}O labeling.²⁰ This P–O stretch is 16 cm^{-1} lower than that in the free ligand, **5**, confirming that the phosphoryl oxygen is coordinated to tungsten.⁸ The FAB mass spectrum of **6** shows a parent ion with the expected isotope pattern as well as peaks from loss of one and two PMePh_2 groups. Loss of the monodentate ligands but no loss of **5** in the mass spectrum also supports a chelated structure for **6**. For **6** prepared from $5\text{-}^{18}\text{O}$, the isotope pattern for the molecular ion is consistent with the expected 60% ^{18}O enrichment (Figure 1).

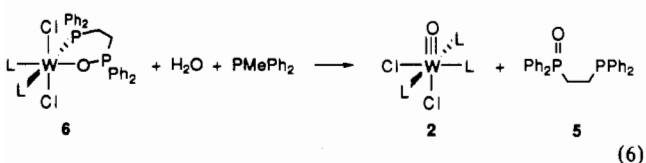
The phosphine oxide ligand in **6** is rapidly displaced from the tungsten by diphos, with the formation of **8** (eq 4; $L = \text{PMePh}_2$).



This is presumably how **8** is formed on thermolysis of **6** (Scheme I). Unlike diphos, PMePh_2 does not efficiently displace **5** from **6**; rather, the equilibrium favors **6** (eq 5; $L = \text{PMePh}_2$). This



is simply the reverse of the reaction of **1** and **5** to form **6**. The fact that the equilibrium favors coordination of **5** is a further indication that it is acting as a chelating ligand. The phosphine oxide ligand is also displaced from **6** on oxidation of the tungsten by water (eq 6; $L = \text{PMePh}_2$). These results support the presence of an intact molecule of **5** complexed to the tungsten center in **6**.



The phosphine oxide **5** is also deoxygenated by $\text{WCl}_2(\text{PMe}_3)_4$ (**9**), the trimethylphosphine analogue of **1**. Heating a benzene

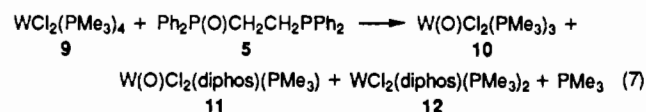
(19) Chatt, J.; Leigh, G. J.; Mingos, D. M. P. *J. Chem. Soc. A* **1969**, 1674–1680. Randall, E. W.; Shaw, D. *J. Chem. Soc. A* **1969**, 2867–2872; *Mol. Phys.* **1965**, *10*, 41. Rossi, R.; Duatti, A.; Magnon, L.; Casellato, U.; Graziani, R.; Toniolo, L. *J. Chem. Soc., Dalton Trans.* **1982**, 1949–1952.

(20) The shift of 21 cm^{-1} on ^{18}O substitution in **6** is less than the 44 cm^{-1} predicted for a simple harmonic oscillator. The shift of 30 cm^{-1} in the free ligand, $5\text{-}^{18}\text{O}$, is also smaller than this predicted value.

Table I. Crystallographic Data for $\text{W}(\text{O})\text{Cl}_2[\text{CH}_2=\text{CHCH}_2\text{P}(\text{O})\text{Ph}_2]\text{PMePh}_2$ (**13**)

$a = 9.2547$ (9) Å	formula $\text{WO}_2\text{Cl}_2\text{P}_2\text{C}_{28}\text{H}_{28}$
$b = 16.738$ (2) Å	fw 713.24
$c = 18.023$ (2) Å	space group $P2_1/c$
$\beta = 100.696$ (9)°	$T = 24\text{ }^\circ\text{C}$
$V = 2743.3$ Å ³	$\lambda = 0.71073$ Å
$Z = 4$	$\rho_{\text{calc}} = 1.727\text{ g cm}^{-3}$
$\mu = 46.363\text{ cm}^{-1}$	transm coeff = 0.9999–0.6929
$R = 0.034$	$R_w = 0.040$
goodness of fit = 1.239	

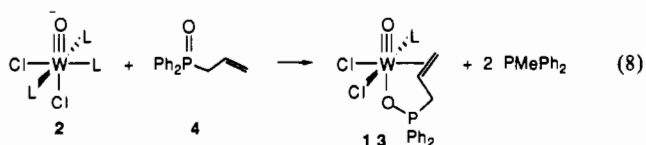
solution of **9** and **5** in a sealed NMR tube at $80\text{ }^\circ\text{C}$ for 2 days yields three tungsten products, analogous to those observed in the reaction of **1** and **5** (eg 7; compare Scheme I). In this case, the



oxo-tris(phosphine) complex **10**¹⁷ is the predominant initial product, rather than the oxo-diphos compound as in the PMePh_2 reactions. On further heating, **12** reacts with any remaining **5** to give additional **10**, **11**, and diphos, shifting the equilibria toward **11** (at 4 days, **10**:**11**:**12** = 1:2:1). An intermediate analogous to **6** is not observed in this reaction, either at ambient temperatures or upon heating (<5% reaction between **5** and **9** is observed after 5 days at $25\text{ }^\circ\text{C}$). Complex **9** is in general much less reactive than **1**, because the PMe_3 ligands dissociate much less readily than PMePh_2 .

In comparison, the simple, nonchelating phosphine oxides Ph_3PO , Ph_2MePO , and Me_3PO are unreactive with **1** over weeks at ambient temperatures. When the reaction mixtures are heated to $70\text{ }^\circ\text{C}$, **1** is substantially decomposed in 1 week, in much the same fashion as occurs in the absence of substrate.¹⁰ Similarly, the slow decomposition of **9** over 1 week at $80\text{ }^\circ\text{C}$ is not significantly perturbed by the presence of Ph_3PO , except perhaps for a slight increase in rate. No oxo products were observed in either case.

Reactions of **1** with the vinyl- and allylphosphine oxides $\text{Ph}_2\text{P}(\text{O})\text{CH}=\text{CH}_2$ (**3**) and $\text{Ph}_2\text{P}(\text{O})\text{CH}_2\text{CH}=\text{CH}_2$ (**4**) are not as clean as the reaction with **5**, forming at least two species in each case. An impure product has been isolated from the reaction of **1** and **4**, which may be a chelated product analogous to **6**, but we have been unable to fully characterize it. The isolated material shows a very complex ^1H NMR spectrum, with roughly 30 overlapping peaks, consistent with the 25 peaks expected for a structure analogous to **6**. A strong band is observed in the IR spectrum at 1124 cm^{-1} , which could be assigned as $\nu(\text{P}-\text{O})$. Heating this material does not appear to yield any oxo complexes. We have examined the reactions of the oxo complex **2** with **4** and with $\text{Ph}_2\text{PCH}_2\text{CH}=\text{CH}_2$ in order to know what the potential reaction products might look like. The former reaction yields an unusual adduct (**13**) as bright yellow crystals (eq 8; $L = \text{PMePh}_2$).



Diamagnetic complex **13** has been characterized by NMR and IR spectroscopies, by FAB mass spectrometry, and by an X-ray crystal structure. It is, to our knowledge, the first isolated complex of ligand **4**. The ^{13}C and ^{31}P NMR spectra of **13** are similar to those of other tungsten(IV)-oxo-alkene complexes we have isolated, although the alkene proton resonances are considerably downfield from those of the related propene complex $\text{W}(\text{O})\text{Cl}_2(\text{CH}_2=\text{CHMe})(\text{PMePh}_2)_2$.¹⁰ It exhibits a P–O stretch at 1126 cm^{-1} in the infrared spectrum, shifted 50 cm^{-1} from that in the free ligand. In CD_2Cl_2 solution in the absence of air, **13** is substantially consumed after 1 week, depositing blue solids, but free phosphine was not observed so it is not clear whether oxygen atom

Table II. Bond Distances (Å) and Angles (deg) in $W(O)Cl_2[CH_2=CHCH_2P(O)Ph_2]PMePh_2$ (13)

W-O(1)	1.702 (4)	W-O(2)	2.177 (3)
W-Cl(1)	2.454 (2)	P(2)-O(2)	1.527 (4)
W-Cl(2)	2.450 (2)	W-C(1)	2.210 (6)
W-P(1)	2.557 (2)	W-C(2)	2.228 (6)
P(1)-C(4)	1.810 (6)	C(1)-C(2)	1.415 (8)
P(1)-C(30)	1.818 (5)	C(2)-C(3)	1.522 (8)
P(1)-C(40)	1.822 (5)	P(2)-C(3)	1.809 (6)
P(2)-C(10)	1.793 (5)	P(2)-C(20)	1.786 (6)
O(1)-W-Cl(1)	102.9 (2)	O(2)-W-Cl(1)	83.18 (9)
O(1)-W-Cl(2)	97.63 (14)	O(2)-W-Cl(2)	86.53 (10)
O(1)-W-P(1)	93.55 (14)	O(2)-W-P(1)	83.97 (9)
O(1)-W-C(1)	91.1 (2)	O(2)-W-C(1)	81.9 (2)
O(1)-W-C(2)	96.1 (2)	O(2)-W-C(2)	79.1 (2)
O(1)-W-O(2)	173.0 (2)	Cl(1)-W-Cl(2)	83.27 (6)
P(1)-W-C(1)	77.2 (2)	Cl(1)-W-P(1)	79.59 (5)
P(1)-W-C(2)	114.0 (2)	P(1)-W-C(1)	153.9 (2)
P(1)-W-Cl(2)	161.25 (5)	Cl(1)-W-C(2)	156.1 (2)
Cl(2)-W-C(1)	116.9 (2)	Cl(2)-W-C(2)	79.8 (2)
C(1)-C(2)-C(3)	120.0 (5)	W-C(1)-H(1a)	120 (4)
W-C(2)-C(3)	116.1 (4)	W-C(1)-H(1b)	116 (4)
C(2)-C(3)-P(2)	108.5 (4)	W-C(2)-H(2)	114 (4)
C(3)-P(2)-O(2)	107.4 (3)	O(2)-P(2)-C(10)	109.6 (2)
W-O(2)-P(2)	121.2 (2)	O(2)-P(2)-C(20)	110.4 (2)
W-C(1)-C(2)	72.1 (4)	W-C(2)-C(1)	70.7 (3)

Table III. Selected Positional and Equivalent Isotropic Thermal Parameters for $W(O)Cl_2[CH_2=CHCH_2P(O)Ph_2]PMePh_2$ (13)

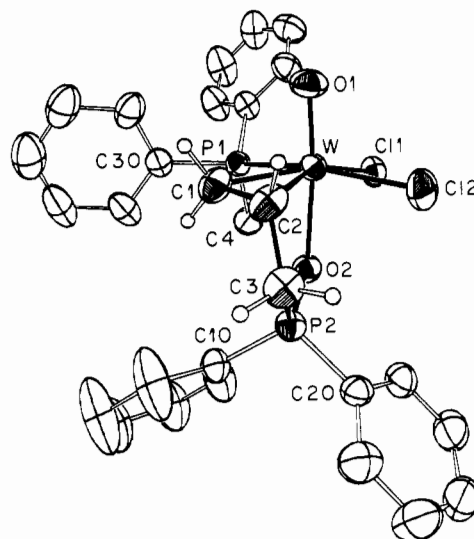
atom	x	y	z	B^a , Å ²
W	0.06157 (3)	0.32589 (1)	0.45930 (1)	3.411 (4)
Cl(1)	0.2802 (2)	0.24717 (10)	0.44805 (9)	4.76 (3)
Cl(2)	0.0513 (2)	0.23518 (11)	0.56486 (9)	5.64 (4)
P(1)	0.1185 (2)	0.38201 (9)	0.33595 (8)	3.44 (3)
P(2)	-0.2139 (2)	0.21356 (10)	0.38625 (8)	3.49 (3)
O(1)	0.1340 (5)	0.4063 (3)	0.5110 (2)	5.0 (1)
O(2)	-0.0525 (4)	0.2329 (2)	0.3866 (2)	3.47 (8)
C(1)	-0.1407 (7)	0.3934 (4)	0.4138 (3)	4.2 (1)
C(2)	-0.1693 (7)	0.3457 (4)	0.4742 (3)	4.3 (1)
C(3)	-0.2719 (7)	0.2742 (4)	0.4585 (3)	4.4 (1)
C(4)	0.1240 (8)	0.3026 (4)	0.2684 (3)	5.0 (2)

^a Anisotropically refined atoms are given in the form of the isotropic equivalent thermal parameter defined as $\frac{1}{3}[a^2\beta_{11} + b^2\beta_{22} + c^2\beta_{33} + ab(\cos \gamma)\beta_{12} + ac(\cos \beta)\beta_{13} + bc(\cos \alpha)\beta_{23}]$.

transfer is involved in the decomposition.

Crystals of **13** contain discrete molecules with a distorted octahedral structure (Figure 2; Tables I-III present crystallographic data, bond lengths and angles, and atomic coordinates). The tungsten is bound to a terminal oxo group, two chlorides, and one $PMePh_2$ ligand in addition to the chelating allylphosphine oxide. The overall geometry and the metrical data are very similar to those of the tungsten-oxo-ethylene complex $W(O)Cl_2(CH_2=CH_2)(PMePh_2)_2$ (**14**).¹⁰ For instance, the tungsten-oxygen multiple-bond distances are essentially the same in the two compounds (1.702 (4) Å in **13**, 1.714 (6) Å in **14**) and the ligands cis to the oxygen are bent away from it (average O(1)-W-L_{cis} = 96.3°). Both features are typical of tungsten-oxo compounds.^{21,22}

The allylphosphine oxide ligand is bound to tungsten through both the alkene and the oxygen, such that the five-membered chelate ring, W-C(2)-C(3)-P(2)-O(2), is essentially perpendicular to the tungsten-alkene plane (the angle between the W-C(1)-C(2) plane and the W-C(2)-C(3)-O(2) least-squares plane is 84.5°). The alkene ligand lies cis and perpendicular to the W=O bond (O(1)-W-C_{alkene} = 91.1 (2), 96.1 (2)°), as in **14**, because it is only in this orientation that tungsten-to-alkene back-bonding can occur.¹⁰ The W-C_{alkene} bond distances in **13** (2.210 (6), 2.228 (6) Å) are similar to those in **14** (2.218 (12), 2.221 (12) Å). The phosphine oxide binds trans to the oxygen

**Figure 2.** ORTEP drawing of $W(O)Cl_2[CH_2=CHCH_2P(O)Ph_2]PMePh_2$ (**13**).

because that is generally the site for the hardest donor in d^2 oxo complexes.²³ Thus, the stereochemistry about tungsten is a result of the electronic requirements of the d^2 metal-oxo center. A similar coordination geometry has been observed for the d^1 oxo complex $Mo(O)Cl_3[Et_2P(O)CH_2CH_2PEt_2]$, with the phosphine ligand cis to the molybdenum-oxo group and the phosphoryl trans.²⁴

The W-O(2) and O(2)-P(2) bond lengths of 2.177 (3) and 1.527 (4) Å are typical of tungsten-phosphine oxide complexes,^{24,25} although the W-O(2)-P(2) angle is unusually small (121.2 (2)° vs 140-165° in other tungsten structures). Small angles have also been observed in complexes of $Et_2P(O)CH_2CH_2PEt_2$ (142.3 (1)°²⁴) and $MePhP(O)C_6H_4PMePh$ (134.9 (3)°^{25a}), both of which contain six-membered chelate rings (similar to the proposed structure of **6**). The angle in **13** is even less than these presumably because of the smaller chelate ring size ($5^{1/2}$, counting to the middle of the alkene).

Discussion

Oxygen atom transfer from the phosphine oxide **5** to tungsten(II) complexes is a remarkable reaction. Phosphines will remove oxygen atoms from a wide variety of metal-oxo complexes because of the strong phosphorus-oxygen bond;^{2,26} these are the first examples of oxygen atom transfer in the reverse direction, from a phosphine oxide to a metal center.⁹ These reactions indicate that the tungsten-oxygen bond in $W(O)Cl_2(PR_3)_3$ is quite strong. We have previously estimated the W=O bond strength in **2** to be greater than 138 kcal/mol, on the basis of the cleavage of CO_2 by **1**.¹²

That oxygen atom transfer is observed only for the bifunctional substrate **5** supports our original hypothesis that deoxygenation of simple phosphine oxides by **1** is thermodynamically favorable, but kinetically difficult because of unfavorable initial binding of the phosphine oxide to tungsten. In the chelate **5**, the phosphine group acts as a tether to bring the phosphine oxide to the metal, thus increasing its local concentration. A similar effect has been

(21) Mayer, J. M. *Inorg. Chem.* **1988**, *27*, 3899-3903.

(22) Reference 3, Chapter 5, especially p 157.

(23) Bryan, J. C.; Stenkamp, R. E.; Tulip, T. H.; Mayer, J. M. *Inorg. Chem.* **1987**, *26*, 2283-2288.

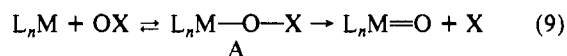
(24) Bakar, M. A.; Hills, A.; Hughes, D. L.; Leigh, G. J. *J. Chem. Soc., Dalton Trans.* **1989**, 1417-1419.

(25) (a) Hall, S. R.; Skelton, B. W.; White, A. H. *Aust. J. Chem.* **1983**, *36*, 267-270. (b) de Wet, J. F.; Cairns, M. R.; Gellatly, B. J. *Acta Crystallogr. B* **1978**, *B34*, 762-766. (c) Kersting, M.; Friebel, C.; Dehnicke, K.; Krestel, M.; Allmann, R. *Z. Anorg. Allg. Chem.* **1988**, *563*, 70-78. (d) Darenbourg, D. J.; Pala, M.; Simmons, D.; Rheingold, A. L. *Inorg. Chem.* **1986**, *25*, 3537-3541. (e) Hill, L. H.; Howlander, N. C.; Mabbs, F. E.; Hursthouse, M. B.; Abdul Malik, K. M. *J. Chem. Soc., Dalton Trans.* **1980**, 1475-1481.

(26) Cf. ref 3, pp 241-244.

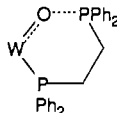
observed in the reactions of **1** with alcohols and ethers: while aliphatic alcohols react only slowly and saturated ethers not at all, reactions of unsaturated substrates (allyl alcohol, but-1-en-4-ol, allyl trimethylsilyl ether) occur within time of mixing.¹³

The observation of an intermediate prior to oxygen atom transfer—the chelate complex **6**—is quite unusual. Such intermediates (A in eq 9) are not typically observed in reactions that involve oxygen atom transfer from a substrate to a metal. The



precursor complex A is usually not seen either because the initial binding of the substrate is unfavorable or because, once formed, the oxygen atom transfer step is facile (or both). The lack of binding of OPR₃ to **1** is an example of an unfavorable initial equilibrium. Rapid oxygen atom transfer in an intermediate such as A is indicated in the oxidation of [Re(Me₃tacn)Cl₂(OPPh₃)]⁺ by DMSO, since DMSO displacement of OPPh₃ is the rate-determining step.²⁷ The lack of observation of an intermediate in the deoxygenation of **5** by **9** may be due to unfavorable initial coordination—an inability of **5** to displace two PMe₃ ligands—since its displacement of the more labile PMePh₂ ligands in **1** is not overly favorable (eq 5). Alternatively, facile oxygen atom transfer may occur in the intermediate—substitution of the PMe₃ ligands in **9** probably requires heating (as necessary for most substrates¹⁸), and the intermediate may not be stable at elevated temperatures.

The stability of the intermediate **6** (decomposition only occurs over hours at 80 °C) indicates that there is also a significant kinetic barrier for oxygen atom transfer from phosphorus to tungsten:



No such barrier is observed in the reactions of **1** with Ph₂MePS and Ph₃AsO. The key difference would seem to be the much stronger bond in phosphine oxides compared to these substrates, which is simply more difficult to break (compare $D(\text{Ph}_3\text{P}-\text{O}) = 127 \text{ kcal/mol}$ vs $D(\text{Ph}_3\text{As}-\text{O}) = 103 \text{ kcal/mol}$ ²⁷). Coordination of **5** has only a small effect on the P–O bond, as its stretching frequency in **6** is only 16 cm⁻¹ lower than that in free **5**. Typically, coordination lowers the P–O stretch by 20–80 cm⁻¹,²⁹ a 50-cm⁻¹ shift is observed in **13**, and a 31–36-cm⁻¹ shift is seen in tungsten(II)–carbonyl–phosphine oxide complexes.¹⁶ The decomposition of **6** would appear to involve cleavage of an essentially intact phosphorus–oxygen bond. Thus, our initial hypothesis, that the kinetic barrier in the reactions with phosphine oxides was due to inability of the phosphine oxide to coordinate, is only partly true. The presence of this second barrier is another reason for the lack of reaction of simple phosphine oxides with **1**, since **1** decomposes readily at 80 °C.²⁸

The reactions of **5** with **1** and **9** produce the same types of products, but the ratios of these products are quite different. For instance, the tungsten(II)–diphos complex is formed in much higher yield in the PMe₃ system. This is because the position of the various equilibria are different, due to the fact that PMe₃ is a much better ligand than PMePh₂. Diphos binds much better to tungsten(IV)–oxo centers than two PMePh₂ ligands, but only roughly as well as two PMe₃ ligands: reaction of diphos with **2** yields exclusively **7**, whereas diphos and **10** gives a mixture of **10** and **11**. On the other hand, more electron-rich W(II) species bind diphos better than PMe₃, PMePh₂, or **5** (eq 4). Thus, any free diphos present in solution as a result of equilibria involving tungsten(IV)–oxo complexes will be consumed by W(II) species.

Because these equilibria favor oxo–tris(phosphine) species more in the PMe₃ case (**10**), significant amounts of **10** and **12** are observed, whereas in the PMePh₂ case, **2** and **8** are minor products or are not seen at all.

The phosphine–phosphine oxide **5** is a reasonable chelating ligand, displacing two PMePh₂ ligands despite the low affinity of tungsten(II) for hard donors. It has been previously observed as a chelating ligand in at least one case and has received attention as a cocatalyst with rhodium in a number of processes.³⁰ Bidentate coordination has also been reported for Et₂P(O)–CH₂CH₂PET₂ and MePhP(O)C₆H₄PMePh, which form similar six-membered rings. To our knowledge, **13** is the first reported complex of the allylphosphine oxide ligand **4**. This is an illustration of the unusual ligand affinities of the d² metal–oxo center, preferring a soft, π-acid ligand cis to the oxo group but a hard donor in the trans position.²³ Complexes of **3** are known, but not in which the ligand is chelated,³¹ perhaps because the chelate ring would be too small. The observation of deoxygenation of **5** but not **3** or **4** may be due to both **5** and diphos being good ligands for tungsten. While **4** binds well to tungsten, we have not observed the allylphosphine to coordinate, possibly because of its small chelate ring size. It is also possible that alkene–phosphine oxides are more difficult to deoxygenate than phosphine–phosphine oxides.

Experimental Section

Reactions were carried out on a vacuum line or in a glovebox under a nitrogen atmosphere. Solvents were dried over calcium hydride (methylene chloride, benzene, pentane, triethylamine) or sodium benzophenone (THF, Et₂O) and transferred immediately prior to use. Deuterated solvents were dried and distilled from activated 4-Å sieves. Column chromatography was performed on silica gel (Merck, 230–400 mesh). The solvents used in chromatography (methylene chloride and ethyl acetate) were used as received. Ph₂PCH=CH₂ (Pressure), Ph₂PCH₂CH=CH₂ (Aldrich), and Ph₂PCH₂CH₂PPh₂ (diphos, Strem) were used as received. Ph₂P(O)CH₂CH=CH₂ (**4**, Organometallics Inc.) was dried by stirring in Et₂O and removal of the volatiles. Ph₂P(O)–CH=CH₂ (**3**) was prepared by hydrogen peroxide oxidation of Ph₂PCH=CH₂.³² Ph₂P(O)CH₂CH₂PPh₂ (**5**) was prepared similarly and purified by column chromatography using methylene chloride and ethyl acetate as the eluents. WCl₂(PMePh₂)₄ (**1**),³³ W(O)Cl₂(PMePh₂)₃ (**2**),¹⁷ W(O)Cl₂(CH₂=CH₂)(PMePh₂)₂ (**14**),¹⁰ WCl₂(PMe₃)₄ (**9**),³³ and W(O)Cl₂(PMe₃)₃ (**10**)¹⁷ have been previously reported. Many reactions were carried out in sealed NMR tubes, usually in C₆D₆. The following description is typical: A 10-mg sample of **6**-¹⁸O and 0.5 mL of C₆D₆ were placed in an NMR tube sealed to a ground-glass joint, which was then evacuated and sealed with a torch. Heating for 14 h at 80 °C yielded ¹⁸O-labeled **2** and **7**. The tube was cut open inside a glovebox, the benzene solution was allowed to evaporate, and an IR spectrum was obtained as a Nujol mull [IR 893 cm⁻¹ (ν(W¹⁸O))]. For the purpose of FAB/MS, 4 mg of diphos was added to convert **2** to **7** (Figure 1).

Microanalyses were performed by Canadian Microanalytical Service Ltd., Vancouver, BC. NMR spectra were taken in C₆D₆, unless otherwise noted, on Varian VXR-300 and Bruker AC-200 and WM-500 spectrometers. Infrared spectra were recorded on a Perkin-Elmer 1604 FT-IR instrument and are reported in cm⁻¹. FAB/MS spectra were acquired by using a VG 70 SEQ tandem hybrid instrument of EBqQ geometry, equipped with a standard saddle-field gun (Ion Tech Ltd., Middlesex, U.K.) producing a beam of xenon atoms at 8 keV and 1 mA. The mass spectrometer was adjusted to a resolving power of 1000, and spectra were obtained at 8 kV and at a scan speed of 10 s/decade. Samples were applied to the FAB target as solutions in benzene, toluene, or methylene chloride. 3-Nitrobenzyl alcohol was used as matrix in the positive-ion FAB/MS mode. Observed isotope patterns for molecular

(27) Conry, R. R.; Mayer, J. M. *Inorg. Chem.* **1990**, *29*, 4862–4867.

(28) Deoxygenation of **5** should be more facile than that of a simple phosphine oxide for a thermodynamic reason as well: removal of oxygen from **5** liberates diphos, a good ligand, which provides an additional driving force.

(29) Reference 8, p 425.

(30) Higgins, S. J.; Taylor, R.; Shaw, B. L. *J. Organomet. Chem.* **1987**, *325*, 285–292. Wegman, R. W.; Abatjoglou, A. G.; et al. *J. Chem. Soc., Chem. Commun.* **1987**, 1891–1892. *Chem. Abstr.* **1986**, *105*, 174788q, 78526g, 78523d, 26125f; **1983**, *99*, 532124u, 198452p. The last reference contains a valuable preparation of **5** and related compounds. Other patents: Huang, I. D.; Westner, A. A.; et al. *Chem. Abstr.* **1987**, *108*, 40088q; **1980**, *94*, 156314g.

(31) Johnson, B. F. G.; Lewis, J.; Postle, S. R. *J. Organomet. Chem.* **1976**, *121*, C7–C9. Welch, F. J.; Paxton, H. J., Jr. U.S. Patent 3 422 079, 1969 (*Chem. Abstr.* **1969**, *70*, 58396v).

(32) Berlin, K. D.; Butler, G. B. *J. Org. Chem.* **1961**, *26*, 2537.

(33) (a) Sharp, P. R. *Organometallics* **1984**, *3*, 1217–1223. (b) Sharp, P. R.; Bryan, J. C.; Mayer, J. M. *Inorg. Synth.*, in press.

ions closely resemble the predicted patterns. The two largest peaks in the molecular envelope are reported as well as the observed fragmentation pattern.

Ph₂P(¹⁸O)CH₂CH₂PPh₂ (5-¹⁸O).³⁰ To a solution of diphos (2.0 g, 5.0 mmol) in 60 mL of CH₂Cl₂ was added by syringe 0.17 mL of H₂¹⁸O (97–98%, Cambridge Isotope), followed by condensation of Br₂ vapor (200 Torr in 400 mL, 4.3 mmol). A white solid began to precipitate. The solution was stirred for 0.5 h and was concentrated to dryness. THF (60 mL) was added, 1.2 mL (8.6 mmol) of triethylamine was syringed in, and the solution was stirred for another 0.5 h. The white precipitate (Et₃NHBr) was filtered out, the THF stripped off, and the residue purified by column chromatography (CH₂Cl₂/EtOAc) to yield 234 mg (13%) of 60% ¹⁸O-enriched **5**: IR 1154 (ν(P¹⁸O)), 1184 cm⁻¹ (ν(P¹⁶O)); ³¹P{¹H} NMR δ 28.11 (d, ³J_{PP} = 48 Hz, P(¹⁸O)), 28.15 (d, ³J_{PP} = 48 Hz, P(¹⁶O)), -12.4 (d, ³J_{PP} = 48 Hz); FAB/MS *m/e* 417 (5-¹⁸O, M + H⁺), 415 (5, M + H⁺).

WCl₂(PMePh₂)₂(Ph₂P(O)CH₂CH₂PPh₂) (6). **1** (500 mg, 0.47 mmol) and **5** (294 mg, 0.71 mmol) were combined in 50 mL of benzene, and the mixture was allowed to stir for 10 min. An immediate color change from orange to red was observed. To remove the liberated phosphine, the solution was concentrated to 5 mL and 35 mL of pentane was added. The resulting precipitate was dissolved in 20 mL of Et₂O, and white **5** was filtered off. Precipitation from Et₂O/pentane gave 158 mg (31%) of paramagnetic, ruby red **6**: ¹H NMR (assignments tentative) δ -7.24 (2 H, br s, PCH₂CH₂P), -4.26 (3 H, s, PCH₃), 7.17 (2 H, t, 7 Hz, H_{para}, partially obscured by C₆H₅), 7.29 (4 H, s, H_{meta}), 8.43 (4 H, d, 7 Hz, H_{meta}), 8.58 (2 H, t, 7 Hz, H_{para}), 9.31 (3 H, br s, PCH₃), 9.48 (4 H, d, 7 Hz, H_{meta}), 9.91 (4 H, d, 7 Hz, H_{meta}), 10.02 (4 H, br s, H_{ortho}), 10.20 (4 H, br s, H_{ortho}), 10.40 (2 H, t, 7 Hz, H_{para}), 10.53 (2 H, t, 7 Hz, H_{para}), 12.21 (4 H, br s, H_{ortho}), 13.11 (4 H, br s, H_{ortho}), 24.16 (2 H, br s, PCH₂CH₂P); IR (Nujol) 1167 (s) (ν(PO)), 1123, 1096, 885, 723 (s), 695 cm⁻¹ (s); FAB/MS *m/e* 1068, 1070 (M⁺), 868, 870 (M⁺ - PMePh₂), 668, 670 (M⁺ - 2PMePh₂). **6-¹⁸O** was prepared as above, with **5-¹⁸O**: IR 1146 cm⁻¹ (ν(P¹⁸O)).

W(O)Cl₂(PMePh₂)₂(diphos) (7). Diphos (175 mg, 0.44 mmol) and **2** (310 mg, 0.36 mmol) were combined in 40 mL of benzene, and the mixture was allowed to stir for 12 h. The solution was concentrated to 5 mL, and 25 mL of pentane was added to precipitate **7**, which was filtered off and washed with 2 × 10 mL of pentane. Precipitation from THF/Et₂O gave 65 mg (22%) of purple-gray **7**. Anal. Calcd for W(O)Cl₂P₂C₃₉H₃₇: C, 53.88; H, 4.34. Found: C, 53.81; H, 4.29. Spectral data are as follows: ¹H NMR δ 2.01 (3 H, d, ²J_{HP} = 9 Hz, PCH₃), 1.90, 2.35, 2.75 (1 H, 1 H, 2 H, m, PCH₂CH₂P), 6.75–7.10 (20 H, m, C₆H₅), 7.50 (2 H, m, C₆H₅), 7.65, 7.96, 8.13, 8.21 (each 2 H, t, 9 Hz, H_{ortho}); ¹³C{¹H} NMR (APT pulse sequence) δ 14.76 (d, ¹J_{CP} = 29 Hz, PCH₃), 30.62 (d of d, ¹J_{CP} = 31 Hz, ²J_{CP} = 7 Hz, Ph₂PCH₂CH₂PPh₂), 38.81 (d of d, ¹J_{CP} = 32 Hz, ²J_{CP} = 7 Hz, Ph₂PCH₂CH₂PPh₂), 125–141 (PC₆H₅); ³¹P{¹H} NMR δ 0.08 (d of d, ²J_{PP} = 5 Hz, 216 Hz, ¹J_{WP} = 345 Hz, PMePh₂), 23.77 (d of d, ²J_{PP} = 18 Hz, 216 Hz, ¹J_{WP} = 334 Hz, H₂CH₂P trans to PMePh₂), 28.28 (d of d, ²J_{PP} = 5 Hz, 18 Hz, ¹J_{WP} = 392 Hz, PCH₂CH₂P cis to PMePh₂); IR 1099, 947 (ν(WO)), 892, 742 (s), 693 cm⁻¹ (s); FAB/MS *m/e* 868, 870 (M⁺), 833, 835 (M⁺ - Cl), 668, 670 (M⁺ - PMePh₂), 633, 635 (M⁺ - PMePh₂ - Cl).

W(O)Cl₂(PMe₃)₂(diphos) (11). **10** (200 mg, 0.40 mmol), diphos (647 mg, 1.63 mmol), and 40 mL of benzene were combined in a glass reaction vessel sealed by a Teflon valve, and the mixture was heated at 80 °C for 12 h. The volatiles were removed, another 40 mL of benzene added, and the process repeated. After four cycles, the solution was concentrated to 5 mL, and 35 mL of pentane was added to precipitate a purple-gray solid. Removal of excess diphos was achieved by a second precipitation from benzene with pentane, repeated washing with excess pentane, and precipitation from benzene with Et₂O, to give 50 mg (17%) of light purple **11**: ¹H NMR δ 1.33 (9 H, d, ²J_{HP} = 9 Hz, P(CH₃)₃), 1.70 (1 H), 2.70 (3 H, both m, PCH₂CH₂P), 6.95, 7.10 (12 H, m, C₆H₅), 7.47, 7.86 (each 2 H, m, H_{ortho}), 8.05, 8.19 (each 2 H, t, 9 Hz, H_{ortho}); ¹³C{¹H} NMR (APT pulse sequence) δ 17.35 (d, ¹J_{CP} = 29 Hz, P(CH₃)₃), 30.32 (d of d, ¹J_{CP} = 30 Hz, ²J_{CP} = 6 Hz, PCH₂CH₂P), 38.03 (d of d, ¹J_{CP} = 33 Hz, ²J_{CP} = 7 Hz, PCH₂CH₂P), 125–145 (PC₆H₅); ³¹P{¹H} NMR

-23.81 (d of d, ²J_{PP} = 6 Hz, 211 Hz, ¹J_{WP} = 374 Hz, PMe₃), 24.90 (d of d, ²J_{PP} = 20 Hz, 211 Hz, ¹J_{WP} = 309 Hz, PCH₂CH₂P trans to PMe₃), 32.36 (d of d, ²J_{PP} = 6 Hz, 20 Hz, ¹J_{WP} = 390 Hz, PCH₂CH₂P cis to PMe₃); IR (Nujol) 1097.0, 952.3 (s, ν(WO)), 863.7 (w), 791.9 (w), 744.3, 694.0; FAB/MS *m/e* 744, 746 (M⁺), 709, 711 (M⁺ - Cl), 668, 670 (M⁺ - PMe₃), 633, 655 (M⁺ - PMe₃ - Cl).

W(O)Cl₂(PMePh₂)₂(Ph₂P(O)CH₂CH=CH₂) (13). **4** (62 mg, 0.26 mmol) and **2** (149 mg, 0.17 mmol) were stirred in 60 mL of benzene until all the solids had gone into solution; the mixture was then allowed to sit for 4 days. The solution, which had lightened in color from mauve to yellow, was concentrated to 30 mL and allowed to sit for 2 more days. The resulting powder was filtered off and washed with 2 × 10 mL of benzene to yield 70 mg (57%) of yellow **13**. Further purification was done by precipitation from CH₂Cl₂/pentane. Anal. Calcd for WO₂Cl₂P₂C₂₈H₂₈: C, 47.15; H, 3.96. Found: C, 47.82; H, 4.28. Spectral data are as follows: ¹H NMR (CD₂Cl₂) δ 2.21 (3 H, d, ¹J_{HP} = 10 Hz, PCH₃), 2.05 (1 H, m), 2.2 (1 H, m, obscured by PCH₃), 4.06 (2 H, m), 5.03 (1 H, d, 15 Hz, all CHH'CH=CHH'), 7.45 (17 H), 7.73 (1 H), 7.93 (2 H, all m, C₆H₅); ¹³C{¹H} NMR (APT pulse sequence) δ 11.94 (d, ¹J_{CP} = 33 Hz, PCH₃), 31.81 (d, ¹J_{CP} = 66 Hz, PCH₂CH=CH₂), 52.92 (d, ¹J_{CP} = 4 Hz, PCH₂CH=CH₂), 60.66 (d, ¹J_{CP} = 8 Hz, PCH₂CH=CH₂), 126–136 (PC₆H₅); ³¹P{¹H} NMR δ 14.76 (d, ²J_{PP} = 5 Hz, ¹J_{WP} = 298 Hz, PMePh₂), 60.90 (d, ²J_{PP} = 5 Hz, Ph₂PO); IR 1212 (w), 1126 (br, ν(PO)), 1062, 966 (s, ν(WO)), 889, 743, 693; FAB/MS *m/e* 712, 714 (M⁺).

X-ray Structure of W(O)Cl₂(PMePh₂)₂(Ph₂P(O)CH₂CH=CH₂) (13). A yellow crystal of **13** grown from W(O)Cl₂(PMePh₂)₂ and Ph₂P(O)CH₂CH=CH₂ in C₆D₆ in an NMR tube was mounted in the air in a 0.3-mm capillary. A total of 6880 reflections in two octants (*hkl, hkl*), with 2θ ≤ 55° were collected at 24 °C on an Enraf-Nonius CAD4 diffractometer using Mo Kα radiation monochromatized with graphite (λ = 0.71037 Å). The systematic absences indicated the space group as P2₁/c. Only a 0.3% decay in intensity was observed during data collection, so no correction was applied. An empirical absorption correction was applied (μ = 46.363 cm⁻¹, transmission factors 0.9999–0.6929, average 0.8973). After corrections for absorption and for Lorentz and polarization effects, 6492 independent reflections were obtained on averaging in P2₁/c. The final data set consisted of 4337 unique observed reflections (*I* > 3σ(*I*), *R*_{av} = 0.013 on *F*_o).

The tungsten atom was located on a Patterson map, and the structure was solved in P2₁/c by least-squares refinements in Fourier syntheses. Allyl hydrogen atoms were located on a difference map and refined isotropically. The remaining hydrogen atoms were fixed in calculated positions. Final full-matrix least-squares refinement converged at *R* = 0.034 and *R*_w = 0.040. All calculations used the SDP/VAX package of programs supplied by the Enraf-Nonius Corp., with scattering factors and anomalous dispersion terms taken from the standard compilations.³⁴ Table II lists selected bond distances and angles; Table III gives the atomic coordinates. Full sets of bond distances and angles as well as positional parameters, equivalent isotropic thermal parameters, anisotropic thermal parameters, selected torsional angles, and least-squares planes are available as supplementary material.

Acknowledgment. We thank Sue Critchlow for invaluable help with the X-ray crystal structure determination, Rasmy Talaat for FAB mass spectra, Lauren Atagi for the preparations of **7** and **8**, Jeffrey Bryan for initial studies in this area, Rebecca Conry for helpful discussions, and the National Science Foundation for financial support.

Supplementary Material Available: For **13**, tables of data collection and refinement details, atom positional and thermal parameters, bond distances and angles, torsional angles, and least-squares planes (8 pages); a listing of observed and calculated structure factors (11 pages). Ordering information is given on any current masthead page.

(34) *International Tables for X-Ray Crystallography*; Kynoch: Bringham, England, 1974; Vol. IV, Tables 2.2B, 2.3.1.